The local B-polarization of the CMB: A very sensitive probe of cosmic defects

Juan García-Bellido [a,b,c], Ruth Durrer [c,*], Elisa Fenu [c], Daniel G. Figueroa [a,b,d], Martin Kunz [c]

[a] *Instituto de Física Teórica CSIC-UAM, Spain*
[b] *Departamento de Física Teórica, Universidad Autónoma de Madrid, Cantoblanco, 28049 Madrid, Spain*
[c] *Département de Physique Théorique, Université de Genève, 24 quai Ernest Ansermet, CH-1211 Genève 4, Switzerland*
[d] *Theory Division CERN, CH-1211 Genève 23, Switzerland*

ABSTRACT

We present a new and especially powerful signature of cosmic strings and other topological or non-topological defects in the polarization of the cosmic microwave background (CMB). We show that even if defects contribute 1% or less in the CMB temperature anisotropy spectrum, their signature in the local $\tilde{B}$-polarization correlation function at angular scales of tens of arc-minutes is much larger than that due to gravitational waves from inflation, even if the latter contribute with a ratio as big as $r \simeq 0.1$ to the temperature anisotropies. We show that when going from non-local to local $\tilde{B}$-polarization, the ratio of the defect signal-to-noise with respect to the inflationary value increases by about an order of magnitude. Proposed B-polarization experiments, with a good sensitivity on arc-minute scales, may either detect a contribution from topological defects produced after inflation or place stringent limits on them. Already Planck should be able to improve present constraints on defect models by about an order of magnitude, to the level of $\epsilon = Gv^2 < 10^{-7}$. A future full-sky experiment like CMBpol, with polarization sensitivities of the order of 1 μK arcmin, will be able to constrain the defect parameter ϵ to less than a few $\times 10^{-9}$, depending on the defect model.

© 2010 Elsevier B.V. Open access under CC BY license.

1. Introduction

Many inflationary models terminate with a phase transition which often also leads to the formation of cosmic strings and other topological defects [1]. Furthermore, we have recently argued [2] that the end of hybrid inflation may involve the self-ordering of an N-component scalar field. Even though for $N > 4$ this does not induce the formation of topological defects, the self-ordering dynamics leads to a scale-invariant spectrum of fluctuations which leaves a signature on the CMB [3,4]. It has been shown long ago that topological defects do not generate acoustic peaks [5] and therefore they cannot provide the main contribution to the CMB anisotropies. However, they still may provide a fraction of about 10%, similar to a possible gravitational wave contribution [6] in the temperature anisotropies of the CMB.

The perturbations from cosmic strings and other topological defects are proportional to the dimensionless variable $\epsilon = Gv^2$ where v is the symmetry breaking scale. For cosmic strings $\mu = v^2$ is the energy per unit length of the string [7]. Present CMB data limit the

contribution from defects [6] such that $\epsilon < 7 \times 10^{-7}$. Stronger limits on ϵ have been derived from the gravitational waves emitted from cosmic string loops [8–10], but these are quite model dependent and will not be discussed here.

In this Letter we show that measuring the local $\tilde{B}$-polarization correlation function of the CMB provides stringent limits on defects or, alternatively, detects them. The physical reason for this is twofold. First, defects lead not only to tensor but also to even larger vector perturbations [4]. What is more important, vector modes generate much stronger B-polarization than tensor modes with the same amplitude, see e.g. [11]. B-polarization is not only a 'smoking gun' for gravitational waves from inflation, but it is also extremely sensitive to the presence of vector perturbations (vorticity). Furthermore, the B-polarization of the angular power spectrum of topological defects, especially of cosmic strings, peaks on somewhat smaller scales than the one from tensors due to inflation. The local $\tilde{B}$-correlation function, which is obtained from the polarization by two additional derivatives, enhances fluctuations on small angular scales. As we shall see, measuring the local $\tilde{B}$ instead of the usual non-local B-correlation function results in an enhancement of the signal to noise ratio from defects with respect to the inflationary one by about a factor 10.

---

* Corresponding author.
  E-mail address: ruth.durrer@unige.ch (R. Durrer).

2. The local $\tilde{B}$-polarization correlation function

Since Thomson scattering is direction dependent, a non-vanishing quadrupole anisotropy on the surface of last scattering leads to a slight polarization of the CMB [11]. This polarization is described as a rank-2 tensor field $\mathcal{P}_{ab}$ on the sphere, the CMB sky. It is usually decomposed into Stokes parameters, $\mathcal{P}_{ab} = (I\sigma_{ab}^{(0)} + U\sigma_{ab}^{(1)} + V\sigma_{ab}^{(2)} + Q\sigma_{ab}^{(3)})/2 = I\delta_{ab}/2 + P_{ab}$, where $\sigma^{(\mu)}$ are the Pauli matrices [11], and I corresponds to the intensity of the radiation and contains the temperature anisotropies. Thomson scattering does not induce circular polarization so we expect $V = 0$ for the CMB polarization, and hence P_{ab} to be real. We define an orthonormal frame $(\mathbf{e}_1, \mathbf{e}_2, \mathbf{n})$ and the circular polarization vectors $\mathbf{e}_\pm = \frac{1}{\sqrt{2}}(\mathbf{e}_1 \pm i\mathbf{e}_2)$, which allows us to introduce the components $P_{++} = 2\mathbf{e}_+^a \mathbf{e}_+^b P_{ab} = Q \pm iU$ and $P_{+-} \propto V = 0$. The second derivatives of this polarization tensor determine the local $\tilde{E}$- and $\tilde{B}$-polarizations,

$$\nabla_- \nabla_- P_{++} + \nabla_+ \nabla_+ P_{--} = 2\nabla_a \nabla_b P_{ab} \equiv \tilde{E},$$

$$\nabla_- \nabla_- P_{++} - \nabla_+ \nabla_+ P_{--} = 2\epsilon_{cd}\epsilon_{ab}\nabla_c \nabla_a P_{bd} \equiv \tilde{B}.$$

Here $\nabla_\pm$ are the derivatives in the directions $\mathbf{e}_\pm$ and ϵ_{cd} is the 2-dimensional totally anti-symmetric tensor. These functions are defined *locally*. The usual E- and B-modes can be obtained by applying the inverse Laplacian to the local $\tilde{E}$- and $\tilde{B}$-polarizations. Such inversions of differential operators depend on boundary conditions which can affect the result for local observations. The $\tilde{B}$-correlation function, $C^{\tilde{B}}(\theta) \equiv \langle \tilde{B}(\mathbf{n})\tilde{B}(\mathbf{n}')\rangle_{\mathbf{n}\cdot\mathbf{n}'=\cos\theta}$, is measurable locally. It is related to the B-polarization power spectrum C_ℓ^B by [11]

$$C^{\tilde{B}}(\theta) = \frac{1}{4\pi}\sum_{\ell=2}^{\infty}\frac{(\ell+2)!}{(\ell-2)!}(2\ell+1)P_\ell(\cos\theta)C_\ell^B. \tag{1}$$

Here $P_\ell(x)$ are the Legendre polynomials. Analogous formulae also hold for $C^{\tilde{E}}$. Note the additional factor $n_\ell = (\ell+2)!/(\ell-2)! = \ell(\ell^2-1)(\ell+2) \sim \ell^4$ as compared to the usual non-local E- and B-polarization correlation functions. At first sight one might argue that whether one expresses a result in terms of C_ℓ^B's or $C_\ell^{\tilde{B}} = n_\ell C_\ell^B$ should really not make a difference since both contain the same information. For an ideal full-sky experiment which directly measures the C_ℓ^B with only instrumental errors this is true. But a CMB experiment usually measures a polarization direction and amplitude with a given resolution over a patch of sky and with a significant noise level. The relation between the theoretical ℓ-space and the experimentally determined sky maps with finite size and finite resolution is not bijective. This makes a big difference as we shall show.

3. Results

In Fig. 1 we show the local $\tilde{B}$-polarization power spectra for tensor perturbations from inflation, cosmic strings, textures and the large-N limit of the non-linear sigma-model. All spectra are normalized such that they make up 10% of the temperature anisotropy at $\ell = 10$. Details of how these calculations are done can be found in [4] for global defects and the large-N limit and in [12] for cosmic strings. A comparison of the non-local B-polarization power spectra for cosmic strings and inflation can be found in [13].

It had already been noted in Refs. [15] and [7] that the B-polarization power spectra for defects are larger than those from inflation for the same temperature anisotropy. Defects peak at
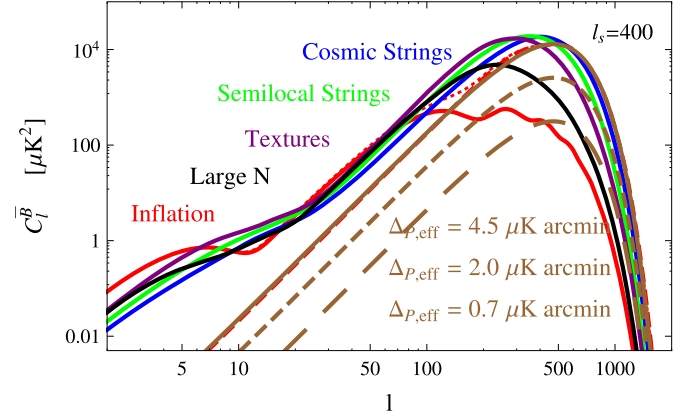

Fig. 1. The local $\tilde{B}$-polarization power spectra for tensor perturbations from inflation, cosmic strings, textures and the large-N limit of the non-linear sigma-model. All spectra are normalized such that they make up 10% of the temperature anisotropy at $\ell = 10$. The dotted red line corresponds to the inflationary contribution taking into account the induced power from lensing of E-modes. The different noise levels (dashed brown curves) precisely mimic the effect of E-lensing. For a definition of the noise amplitude $\Delta_{P,\text{eff}}$ and the smoothing scale ℓ_s see the text. (For interpretation of the references to colors in this figure the reader is referred to the web version of this Letter.)
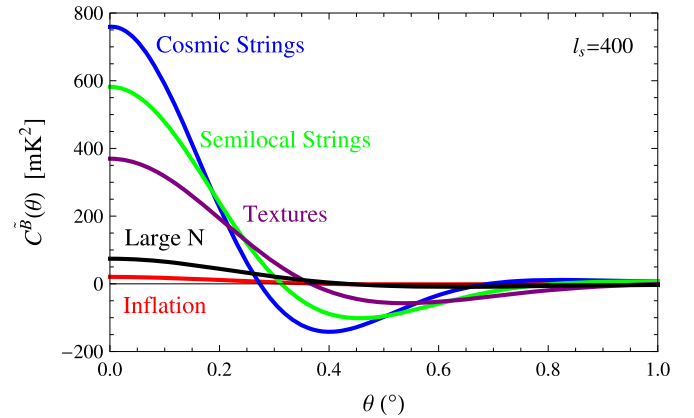

Fig. 2. The local $\tilde{B}$-polarization angular correlation functions for $\theta < 1°$ for inflation and the defect models of Fig. 1, with a smoothing scale $l_s = 400$.

somewhat higher ℓ's than inflationary perturbations, since B-modes from defects are dominated by their vector (vorticity) modes. This contribution is maximal on scales that are somewhat smaller than the horizon scale, while gravitational waves truly peak at the Hubble horizon at decoupling, which corresponds to $\ell \sim 100$. As a consequence, the *local* $\tilde{B}$-polarization spectra for defects are even larger than those from inflation because of the factor $n_\ell \simeq \ell^4$. This is most pronounced for cosmic strings, which have considerable power on small scales, but it is also true for other defects.

Due to the extra factor n_ℓ, in the local $\tilde{B}$-power spectra shown in Fig. 1, power at small scales (high ℓ) counts significantly more than power at larger scales (low ℓ). For this reason defect models dominate over the inflationary B-modes of the same amplitude. This is seen very prominently in the 2-point angular correlation function shown in Fig. 2 where we can compare the defect peaks coming from cosmic strings, textures and large-N. Note the decreasing height but increasing width of the peak as we go from cosmic strings to large-N models.

For $0.2 < \theta < 1°$, where the inflationary $\tilde{B}$-polarization is about -2 mK^2, that from cosmic strings is -150 mK^2, nearly a factor 100 larger. For textures and the large-N model, the difference is

somewhat smaller, roughly a factor of 50 and 10 respectively. The very pronounced peak on very small scales is not visible due to the noise.

Even though constructed ad hoc, coherent causal seed models (but not topological defects) can have acoustic peaks, see Ref. [18], which thus cannot be used as a differentiating signature from inflation. But the fact that polarization is generated at the last scattering surface implies that it cannot have power on scales larger than the horizon at decoupling, corresponding to about $\ell \sim 100$, or angles $\theta > 2°$, unless something like inflation has taken place [16]. This can only be circumvented if one allows for acausality, i.e. superluminal motion, of the seeds [19], however improbable. In Ref. [20] the authors have shown that this superhorizon signature appears not only in the TE-cross correlation spectrum, but also in the local $\tilde{B}$-polarization spectrum. We find that this is somewhat weakened by re-ionization, which adds power on large scales to the B-polarization from defects, see Fig. 1.

4. Observational prospects

It is clear from Fig. 2 that cosmic defects with equal amplitude as the tensor component from inflation (note $\epsilon = 7 \times 10^{-7}$ is equivalent to $r = 0.1$) would have a significant peak in the two-point correlation function of the local $\tilde{B}$-polarization, on angular scales of order tens of arc-minutes. A relevant issue is whether this peak could be measured with full-sky probes like Planck [21] or CMBpol [22], or even with small-area experiments. This is difficult because, although CMB experiments typically have a flat (white) noise power spectrum for the Stokes parameters, the local $n_\ell \sim \ell^4$ factor induces a very blue spectrum for the noise in the local $\tilde{B}$-modes, which erases the significance of the broad defect peak at $\ell \sim 500$ in the $C_\ell^{\tilde{B}}$ power spectrum. Moreover, in order to extract the cosmological $\tilde{B}$-polarization signal it is necessary first to clean the map from the contribution coming from gravitationally lensed $\tilde{E}$-modes. This induces an extra 'lensing noise' $\Delta_{P,\text{eff}} \sim 4.5$ μK arcmin for uncleaned maps that can be reduced to $\sim (0.1$–$0.7)$ μK arcmin by iterative cleaning or a simple quadratic estimator respectively [14]. Furthermore, CMB experiments have an angular resolution determined by the microwave horn beam width, θ_{FWHM}, which induces an uncertainty in the C_ℓ's that can be described by an exponential factor $\exp[\ell(\ell+1)\sigma_b^2]$, with $\sigma_b = \theta_{\text{FWHM}}/\sqrt{8\log 2}$. Resolutions of order 10 arc-minutes, like those of the Planck HFI experiment, correspond to multipoles $\ell_b = 1/\sigma_b \sim 800$. Adding the steep polarization noise, with typical amplitude $\Delta_{P,\text{eff}} = (0.5$–$12)$ μK arcmin, would make the signal disappear under the small-scale noise. In order to regulate this divergence, we smooth both the signal and the noise with a Gaussian smoothing of width σ_s, corresponding to a smoothing scale $\ell_s < \ell_b$. We choose $\ell_s = 400$ in our analysis.

In order to compute the signal-to-noise ratio S/N for detection of the defect peak in the local $\tilde{B}$-correlation function, we split the interval $\theta \in [0, 1°]$ in 10 equal bins.[1] We then evaluate the theoretical correlation function at the center of those bins, $\mathsf{S}_i = C^{\tilde{B}}(\theta_i)$, and write the covariance matrix of the correlated bins as

$$\mathsf{C}_{ij} = \sum_\ell \frac{2\ell+1}{8\pi^2 f_{\text{sky}}} \left(\mathcal{C}_\ell^{\tilde{B}}\right)^2 P_\ell(\cos\theta_i) P_\ell(\cos\theta_j),$$

where the covariance matrix in ℓ-space is assumed to be diagonal, $\text{cov}[\mathcal{C}_\ell^{\tilde{B}}, \mathcal{C}_{\ell'}^{\tilde{B}}] = 2(\mathcal{C}_\ell^{\tilde{B}})^2 \delta_{\ell\ell'}/(2\ell+1) f_{\text{sky}}$, with $\mathcal{C}_\ell^{\tilde{B}} = (C_\ell^{\tilde{B}} + N_\ell) \exp[-\ell(\ell+1)/\ell_s^2]$. Here f_{sky} is the fraction of the observed

---

[1] Note that Planck has this resolution only for the higher frequency bands, above 200 GHz, where the sensitivity is somewhat reduced.
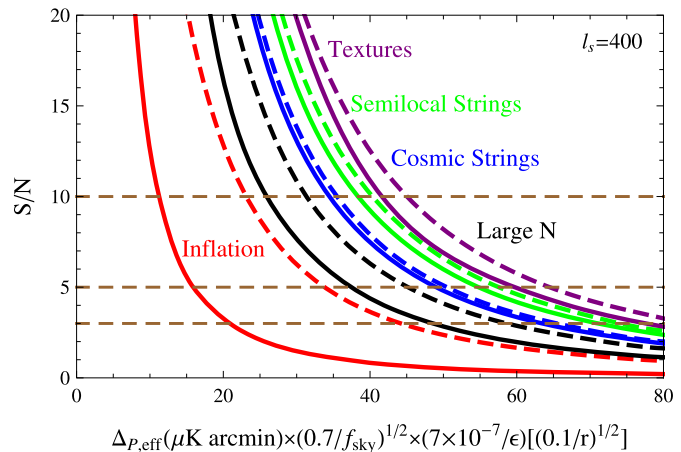

Fig. 3. The signal-to-noise ratio as a function of the normalized polarization sensitivity, for for (from left to right) inflation, large-N limit, cosmic strings, non-local cosmic strings and textures. Solid curves: using angular scales up to 1° and dashed curves: using angular scales up to 4°, with 6 arcmin resolution bins.

Table 1
The limiting amplitude, $\epsilon = Gv^2$, of various defects, at 3-σ in the range $\theta \in [0, 1°]$, for Planck ($\Delta_{P,\text{eff}} = 11.2$ μK arcmin), CMBpol-like exp. ($\Delta_{P,\text{eff}} = 0.7$ μK arcmin) and a dedicated CMB experiment with ($\Delta_{P,\text{eff}} = 0.01$ μK arcmin). We set $f_{\text{sky}} = 0.7$.

$S/N = 3$	Strings	Semi-local	Textures	Large-N
Planck	1.2×10^{-7}	1.1×10^{-7}	1.0×10^{-7}	1.6×10^{-7}
CMBpol	7.7×10^{-9}	6.9×10^{-9}	6.3×10^{-9}	1.0×10^{-8}
$\tilde{B}$ exp.	1.1×10^{-10}	1.0×10^{-10}	0.9×10^{-10}	1.4×10^{-10}

sky which we set to 0.7 for satellite probes. The signal-to-noise ratio for the defect model is $S/N = \sqrt{\mathsf{S}_i \mathsf{C}_{ij}^{-1} \mathsf{S}_j}$. In Fig. 3 we show this ratio as a function of the normalized polarization sensitivity for all types of defects as well as for inflation (where $7 \times 10^{-7}/\epsilon$ has to be replaced by $\sqrt{0.1/r}$). The horizontal lines correspond to 3, 5 and 10-σ respectively. To show why the choice of $\theta_{\text{max}} = 1°$ is optimal we also plot (dashed lines) the S/N for $\theta_{\text{max}} = 4°$, at fixed resolution (6'). For the latter, the noise level allowed for a 3-σ detection increases by more than a factor of 2 for inflation while it does not change much for defects. This behaviour is a telltale sign for defects, and shows that their signal is strongly localised in the angular correlation function, which distinguishes them e.g. from inflationary tensor perturbations and lensed E-modes: the S/N curve from defects does not change much for angles above $\sim 1°$, while the one from inflation increases significantly.

In Table 1 we give the values of ϵ which are measured at 3-σ by Planck (assuming $\Delta_{P,\text{eff}} = 11.2$ μK arcmin [20], where the de-lensing error is added in quadrature), a CMBpol-like experiment with polarization sensitivity $\Delta_{P,\text{eff}} = 0.7$ μK arcmin, and a dedicated CMB experiment with $\Delta_{P,\text{eff}} = 0.01$ μK arcmin. Note, however, that it is not clear how to perform the de-lensing of the B-modes to the level of precision needed for the last case.

In Fig. 4 we show the ratio of S/N from defects to the one from inflation for non-local (dashed) and local $\tilde{B}$-modes (solid curves). In the local polarization the defect signal is substantially enhanced with respect to the inflationary one; by a factor of 5 for large-N models and by 10, 12 and 15 for cosmic strings, semi-local strings and textures respectively. We prefer to show this ratio rather than the absolute local versus non-local S/N curves, since the latter depend sensitively on the assumptions made on the degradation of S/N when going from local to the non-local B-polarization. Something which certainly depends on sky coverage but probably also on other experimental details (e.g. geometry). For the ratio we just
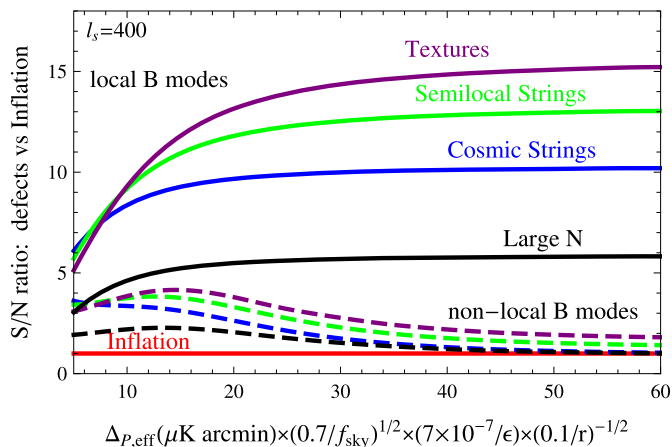
Fig. 4. The ratio of the signal-to-noise from defects to the one from inflation. Solid curves: measuring the local $\tilde{B}$-correlation function. Dashed curves: measuring the non-local B-correlation function.

assume that this degradation is the same for the inflationary and the defect signal.

It is interesting to note that actually textures fare better than cosmic strings even though they have less power on small scales. The reason is that the very small scales are dominated by noise and the signal mainly comes from the intermediate scales around $0.3°$ where textures dominate, see Fig. 2.

5. Conclusions

In this Letter we have shown that measuring the local $\tilde{B}$-polarization correlation function on small scales, $\theta \lesssim 1°$ is a superb way to detect topological and non-topological defects, or alternatively to constrain their contribution to the CMB. For simple inflationary models which lead to defect formation at the end of inflation, a value of $\epsilon \simeq 10^{-7}$–10^{-8} seems rather natural, hence the achieved limits include the relevant regime. The fact that the local $\tilde{B}$-polarization from defects is dominated by the vector mode, which peaks on scales smaller than the horizon, is responsible for a significant enhancement of the local $\tilde{B}$-polarization correlation function on tens of arc-minute scales.

Even though the Planck satellite is not the ideal probe for constraining these models, if it finally reaches down to $r \leqslant 0.025$, see Ref. [17], it will either lead to the detection of a defect contribution, or it will constrain it to $\epsilon = Gv^2 \lesssim 10^{-7}$, depending on the

defect model (textures being the most constrained and large-N non-topological defects the least). Future CMB experiments, with 0.1 arc-minute resolution and sensitivities at the level of 0.1 μK in polarization, could in principle reach the bound $\epsilon < 10^{-10}$ for most defect types, which would rule out a large fraction of present models.

Acknowledgements

References

[1] R. Jeannerot, J. Rocher, M. Sakellariadou, Phys. Rev. D 68 (2003) 103514;
J. Rocher, M. Sakellariadou, JCAP 0503 (2005) 004.
[2] E. Fenu, D.G. Figueroa, R. Durrer, J. Garcia-Bellido, JCAP 0910 (2009) 005.
[3] R. Durrer, M. Kunz, Phys. Rev. D 55 (1997) 4516.
[4] R. Durrer, M. Kunz, A. Melchiorri, Phys. Rev. D 59 (1999) 123005.
[5] R. Durrer, A. Gangui, M. Sakellariadou, Phys. Rev. Lett. 76 (1996) 579.
[6] U. Seljak, A. Slosar, Phys. Rev. D 74 (2006) 063523;
N. Bevis, et al., Phys. Rev. Lett. 100 (2008) 021301;
N. Bevis, et al., Phys. Rev. D 76 (2007) 043005;
L. Pogosian, M. Wyman, Phys. Rev. D 77 (2008) 083509;
J. Urrestilla, et al., JCAP 0807 (2008) 010.
[7] R. Durrer, M. Kunz, A. Melchiorri, Phys. Rep. 364 (2002) 1.
[8] T. Vachaspati, A. Vilenkin, Phys. Rev. D 30 (1984) 2036.
[9] R. Durrer, Nucl. Phys. B 328 (1989) 238.
[10] F. Jenet, et al., Astrophys. J. 653 (2006) 1571.
[11] R. Durrer, The Cosmic Microwave Background, Cambridge University Press, 2008.
[12] N. Bevis, et al., Phys. Rev. D 75 (2007) 065015.
[13] J. Urrestilla, et al., Phys. Rev. D 77 (2008) 123005.
[14] U. Seljak, C. Hirata, Phys. Rev. D 69 (2004) 043005.
[15] U. Seljak, U. Pen, N. Turok, Phys. Rev. Lett. 79 (1997) 1615.
[16] D.N. Spergel, M. Zaldarriaga, Phys. Rev. Lett. 79 (1997) 2180.
[17] ESA document 'Planck-incAnnexes' on the r-limit from 4 sky coverages.
[18] N. Turok, Phys. Rev. Lett. 77 (1996) 4138.
[19] S. Scodeller, M. Kunz, R. Durrer, Phys. Rev. D 79 (2009) 083515.
[20] D. Baumann, M. Zaldarriaga, JCAP 0906 (2009) 013.
[21] The ESA satellite Planck launched in Mai 2009, http://www.esa.int/esaSC/120398_index_0_m.html.
[22] CMB polarization satellite project, http://cmbpol.uchicago.edu/.